STIM1 R304W in mice causes subgingival hair growth and an increased fraction of trabecular bone

Thilini H. Gamage[a,1], Emma Lengle[a,1], Gjermund Gunnes[b], Helen Pullisaar[c], Asbjørn Holmgren[a], Janne E. Reseland[d], Else Merckoll[e], Stefania Corti[f,g], Masahiro Mizobuchi[h], Raul J. Morales[i], Leonidas Tsiokas[j], Geir E. Tjønnfjord[k], Rodrigo S. Lacruz[l], Staale P. Lyngstadaas[d], Doriana Misceo[a,2], Eirik Frengen[a,*,2]

[a] Department of Medical Genetics, Oslo University Hospital and University of Oslo, Oslo, Norway
[b] Faculty of Veterinary Medicine, Norwegian University of Life Sciences, Norway
[c] Department of Orthodontics, Institute of Clinical Dentistry, University of Oslo, Oslo, Norway
[d] Department of Biomaterials, Institute of Clinical Dentistry, University of Oslo, Oslo, Norway
[e] Department of Radiology and Nuclear Medicine, Oslo University Hospital, Oslo, Norway
[f] Neurology Unit, Fondazione IRCCS Ca' Granda Ospedale Maggiore Policlinico, Milan, Italy
[g] Neuroscience Section, Department of Pathophysiology and Transplantation, Dino Ferrari Centre, University of Milan, Milan, Italy
[h] Department of Neurology, Nakamura Memorial Hospital, Sapporo, Japan
[i] CHRU, Hôpital Gui de Chauliac, Montpellier, France
[j] Department of Cell Biology, University of Oklahoma Health Sciences Center, Oklahoma, USA
[k] Department of Haematology, Oslo University Hospital and Institute of Clinical Medicine, University of Oslo, Oslo, Norway
[l] Department of Basic Science and Craniofacial Biology, New York University College of Dentistry, New York, USA

ARTICLE INFO

Keywords:
Abnormal bone architecture
Ectopic hair growth
Skeletal defects
STIM1 R304W
Stormorken syndrome

ABSTRACT

Calcium signaling plays a central role in bone development and homeostasis. Store operated calcium entry (SOCE) is an important calcium influx pathway mediated by calcium release activated calcium (CRAC) channels in the plasma membrane. Stromal interaction molecule 1 (STIM1) is an endoplasmic reticulum calcium sensing protein important for SOCE.

We generated a mouse model expressing the STIM1 R304W mutation, causing Stormorken syndrome in humans. Stim1$^{R304W/R304W}$ mice showed perinatal lethality, and the only three animals that survived into adulthood presented with reduced growth, low body weight, and thoracic kyphosis. Radiographs revealed a reduced number of ribs in the Stim1$^{R304W/R304W}$ mice. Microcomputed tomography data revealed decreased cortical bone thickness and increased trabecular bone volume fraction in Stim1$^{R304W/R304W}$ mice, which had thinner and more compact bone compared to wild type mice. The Stim1$^{R304W/+}$ mice showed an intermediate phenotype. Histological analyses showed that the Stim1$^{R304W/R304W}$ mice had abnormal bone architecture, with markedly increased number of trabeculae and reduced bone marrow cavity. Homozygous mice showed STIM1 positive osteocytes and osteoblasts. These findings highlight the critical role of the gain-of-function (GoF) STIM1 R304W protein in skeletal development and homeostasis in mice. Furthermore, the novel feature of bilateral subgingival hair growth on the lower incisors in the Stim1$^{R304W/R304W}$ mice and 25 % of the heterozygous mice indicate that the GoF STIM1 R304W protein also induces an abnormal epithelial cell fate.

1. Introduction

Calcium signaling plays an important role in bone development and homeostasis [1]. One important Ca^{2+} entry pathway in non-excitable cells is the store-operated Ca^{2+} entry (SOCE) [2,3]. SOCE is mediated by stromal interaction molecule 1 (STIM1), a single-pass transmembrane protein, which resides in the endoplasmic reticulum (ER) membrane and senses ER Ca^{2+} levels [4]. When ER Ca^{2+} stores are low,

* Corresponding author.
E-mail address: eirik.frengen@medisin.uio.no (E. Frengen).
[1] These authors contributed equally to this work.
[2] These authors contributed equally to this work.

STIM1 oligomerizes and translocates to ER-plasma membrane (ER-PM) junctions [5,6]. At these junctions, STIM1 interacts with ORAI1, a tetra-spanning PM protein. ORAI1 forms the ion-conducting pore of the Ca^{2+} release-activated Ca^{2+} channel (CRAC) and enables Ca^{2+} influx across PM [2,3,7–9]. The study of patients and mouse models with mutations in *ORAI1* or *STIM1* genes contribute to the understanding of the function of these proteins through phenotypes related to dysregulated SOCE [8,10–15].

Mutations in the *ORAI1* or *STIM1* genes cause diseases in human [9–11,13–15]. Bi-allelic loss-of-function (LoF) mutations in *STIM1* or *ORAI1* result in absence of SOCE and patients present with Immunodeficiency 10 (IMD10, OMIM #612783) or Immunodeficiency 9 (IMD9, OMIM #612782) [12,15], respectively. The clinical presentation includes immunodeficiency, autoimmunity, ectodermal dysplasia, muscular hypotonia, and severe dental enamel defects, which highlights the role of CRAC in tooth development [8,9,12,15–17]. Heterozygous gain-of-function (GoF) mutations in *STIM1* and *ORAI1* in humans cause constitutive SOCE resulting in a spectrum of diseases ranging from isolated tubular aggregate myopathy (TAM) (TAM1, OMIM #160565, TAM2, OMIM #615883) to Stormorken syndrome (STRMK, OMIM #185070) [15–18]. Stormorken syndrome, caused by the *STIM1* c.910C > T; p.R304W mutation, is a rare multi-organ disease, presenting with tubular aggregate myopathy, fatigue, anemia, thrombocytopathy, thrombocytopenia, miosis, asplenia, ichthyosis, and headache [10,13,14,18–20]. Interestingly, the effect of GoF STIM1 mutations in the skeletal or dental tissues has not been explored in patients with TAM or Stormorken syndrome [13,14,18,20–23].

Stim1$^{-/-}$ and *Orai1*$^{-/-}$ mouse models have provided insight into the effects of absent SOCE and the resulting cellular Ca^{2+} dysregulation [24–28]. These mice present with neonatal lethality, where the surviving mice from both knock-out models displayed significantly reduced growth [24,26–28]. In addition, the *Orai1*$^{-/-}$ mice presented with a severe osteoporotic bone phenotype, characterized by a decreased bone volume versus tissue volume and decreased trabecular number and increased trabecular spacing [26].

On the other hand, mouse models expressing STIM1 GoF mutations causing constitutive SOCE also manifested pathological features [29–31]. Heterozygous *Stim1*^{Sax} mice expressing the STIM1 EF-hand mutation D84G [30], which causes TAM1 in humans [10], developed spleen abnormalities including increased spleen size and abnormal red and white pulp architecture. The *Stim1*^{Sax} mice also show bone marrow fibrosis and increased collagen deposition which affected the femoral bone cavity in heterozygous state [30]. Two mouse models expressing STIM1 R304W have been reported [29,31]. Both models are described with reduced body size, hematological and muscular defects, and homozygous lethality. The *Stim1*^{R304W} model described by Silva-Rojas et al., also displayed spleen enlargement, reduced bone marrow cavity, abnormal cortical and trabecular architecture and diminished bone strength [31].

In this paper, we extend the phenotyping of our mouse line expressing the STIM1 R304W mutation, named Stim1^{R304W} [29], to further elucidate the abnormalities in the skeletal system due to constitutive SOCE. We describe macroscopic skeletal anomalies and severe changes in the bone architecture in the Stim1^{R304W} mice, as well as a novel feature of ectopic subgingival hair growth on the labial side of the lower incisors.

2. Methods

2.1. Maintenance of mice

All animals were housed at standard conditions (12:12-hr light/dark, 21 ± 2 °C temperature and 55 ± 5 % relative humidity) with *ad libitum* access to water and standard chow. All animal experimental protocols for generation, breeding and use of transgenic animals in Norway were registered and approved by the Norwegian Food Safety Authority (Mattilsynet, Experimental animal welfare supervision and application system ID 7216 and 6991) and followed the ethical guidelines given in Directive 2010/63/EU of the European Parliament on the protection of animals used for scientific purposes.

The Stim1^{R304W} mouse model carrying the *Stim1* (NC_000073.6) chr7:102421471A > T (GRCm38.p4) mutation, resulting in a R304W amino acid substitution in STIM1 was established by Gamage et al. [29]. The mouse line was generated on a C57bl6xCBA F1 background using Zinc Finger technology [29]. All animals in the study were euthanized at 5–6 months of age and a full necropsy was performed. Tissues were stored in 10 % formalin or snap frozen until further analysis.

2.2. Spleen measurement

Total body weight was measured in live animals before euthanasia. Upon euthanasia, the spleen of each animal was dissected, photographed, weighed and length measured. The size of spleen is presented as a ratio of spleen and total body mass at euthanasia.

2.3. Whole mouse radiographs

Whole animal radiography of formalin fixed mice was performed using Philips X-ray generator and tube (Philips Norge AS, Health Systems,Oslo, Norway) and Sound Eklin DR developer (Medivet Scandinavian AB, Ängelholm, Sweden).

2.4. Microcomputed tomography (μCT) analysis of the tibia

Microcomputed tomography (μCT) scanning was performed to measure morphological indices of metaphyseal regions of tibias. Formalin fixed bone samples wrapped in plastic foil were rotated around their long axes with a rotation step of 0.4° and images were acquired using Bruker Skyscan 1172 (Bruker, Kontich, Belgium) with the following parameters: pixel size =5 μm; peak tube potential =100 kV; X-ray intensity =100 μA; 0.5-mm aluminum filter. Raw images were reconstructed by the NRecon Reconstruction Software (Microphotonics, Inc. Allentown, PA) to 3-dimensional cross-sectional image data sets, using a 3-dimensional cone beam algorithm. For the reconstruction, beam hardening was set to 0 %, smoothing to 1, and ring artefact reduction to 10. Structural indices were calculated on reconstructed images using the CT-Analyser (CTAn) software package (Blue Scientific Limited, Cambridge, UK). Cortical and trabecular bone were separated using a custom processing algorithm in CTAn, based on the different thicknesses of the structures. Cortical bone was analyzed by a region of 180 slices, starting 9 mm distal to the metaphysis. Cortical parameters included mean total cross sectional area, cortical bone volume and cortical bone area. Trabecular bone was analyzed in the proximal metaphysis region, starting just distal to the metaphysis and continued distally for 240 slices. Trabecular parameters included trabecular separation, trabecular bone volume fraction and trabecular number.

2.5. Histology

Formalin fixed tibiae from Stim1$^{+/+}$ and Stim1$^{R304W/R304W}$ mice, were decalcified in a decalcification solution (34 g Sodium formate (HCOONa), 151 ml concentrated formic acid, 1 L H_2O) for 24 h and paraffin embedded. The tissue blocks were then sectioned at 4 μm thickness and stained with hematoxylin and eosin (HE) using standard protocols.

2.6. Immunohistochemistry

Adjacent sections obtained from tissue block sectioning were stained for STIM1 using the avidin-biotin method with the Vectastain

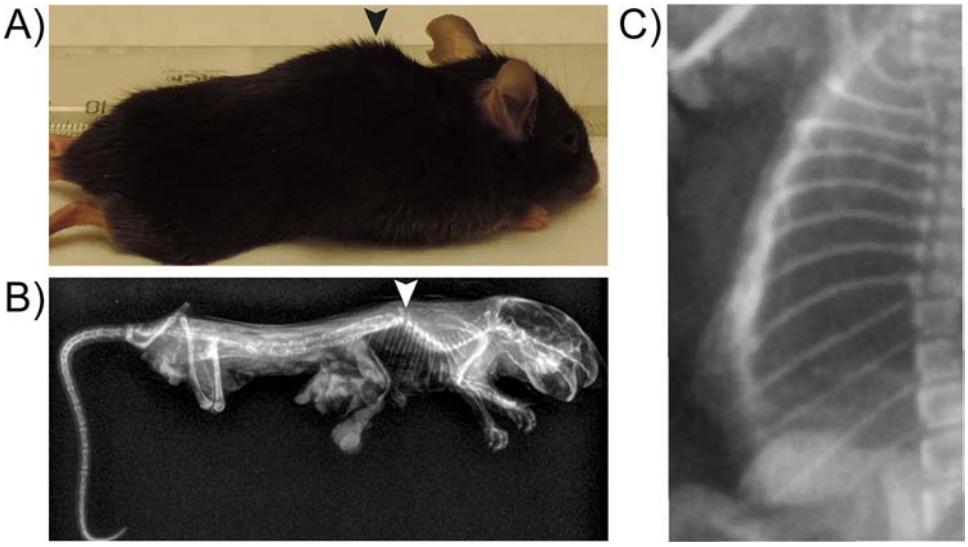

Fig. 1. Thoracic kyphosis and 12 pairs of ribs in the Stim1$^{R304W/\ R304W}$ mice.
(A–B) Lateral view of a representative Stim1$^{R304W/R304W}$ mouse showing thoracic kyphosis (arrowhead) (A), confirmed by whole body X-ray (B).
(C) Representative image of a chest X-ray from Stim1$^{R304W/R304W}$ mouse showing 12 pairs of ribs.

Elite ABC System (PK-6100, Vector Laboratories, Burlingame, CA, USA). Sections were de-paraffinized and antigen retrieval performed at 92 °C for 5 min, in citrate buffer (0.01 M, pH 6.0) followed by a 5 min incubation in the heated solution. Sections were rinsed in distilled H_2O and the process was repeated, followed by 15 min incubation in the heated solution and 15 min incubation in 3 % H_2O_2 in methanol/distilled H_2O, and stored overnight at 4 °C in phosphate buffered saline (PBS). The sections were blocked for 30 min in 1:100 normal goat serum in PBS and stained with 1:400 anti-human STIM1 (LS-C209377, LifeSpan BioSciences, Inc., Seattle WA, USA) for 1 h at room temperature on a rotating table followed by a 30 min incubation with 1:50 biotinylated goat anti-rabbit antibody (Vectastain kit). Samples were washed and treated with avidin (1:50 in PBS) and biotinylated horseradish peroxidase (1:50 in PBS), for 30 min at room temperature followed by rinse with PBS with 0.05 % Tween 20. The STIM1 signal was developed for 8 min with ImmPACT AEC (SK-4205, Vector Laboratories). The sections were subsequently contrast stained with hematoxylin and mounted in xylene.

2.7. Macroscopy and scanning electron microscopy (SEM) of mouse dental structures

All animals aged 5 weeks to 6 months were examined macroscopically for presence of ectopic subgingival hair growth below the lower central incisors. Jaws were dissected at euthanasia at 5–6 months age, stored in formalin and or PBS and shipped at room temperature to NYU College of Dentistry for Backscattered Scanning Electron Microscopy (BSE-SEM) analysis as reported previously [32]. Briefly, mandibles of WT and Stim1^{R304W} mice were extracted and cleared of soft tissues, dehydrated, embedded in PMMA resin before sectioning about 2 mm from the incisor tip. After polishing, samples were imaged in parallel in the BSE-SEM without conductive coating setting contrast and brightness to the WT sample.

2.8. Re-analysis of X-rays and computed tomography (CT) scans from patients with Stormorken syndrome

Available radiographs from patients F1 III-1, F2 II-3, F3 II-1 and F4 III-1 described by Misceo et al., [13] were collected and assessed retrospectively. Images collected include: computed tomography (CT) of the neck, chest and abdomen of F1 III-1; CT of the head and radiographs of chest, hands and lower extremities in F2 II-3; radiographs of cervical spine and lower extremities in F3 II-1; and finally, CT of the head, chest and abdomen and radiographs of the spine of F4 III-1 (numbers as previously reported). Chest X-rays from patient F1 III-2 described by Nesin et al., [14] and the patient described by Borsani et al. [33], were also assessed.

2.9. Statistics

Statistical analyses of μCT parameters were performed using the SPSS Statistics software (IBM Corp. Released 2017. IBM SPSS Statistics for Windows, Version 25.0. Armonk, NY: IBM Corp.). Exact significance was tested based on Mann-Whitney *U* test (2-tailed) to compare the differences between groups. A p-value < 0.05 was defined as statistically significant. Student's *t*-test (unpaired) was used to evaluate significant differences in the spleen to body mass ratios.

3. Results

3.1. Stim1$^{R304W/\ R304W}$ mice showed thoracic kyphosis and reduced number of ribs

A knock-in mouse line expressing the STIM1 R304W mutation was established [29]. This resulted in perinatal lethality in homozygous state. Only three homozygous mice survived into adulthood following 25 heterozygous crosses, which in total resulted in 130 offspring. The surviving mice presented with reduced growth and body size compared to age and sex matched wild type littermates [29].

The three homozygous mice were euthanized at 5–6 months of age and stored in formalin before the examination of the skeletons. Macroscopic examination of the mice revealed thoracic kyphosis, which was further documented by whole body X-ray radiographs (Fig. 1A–B). The radiographs also revealed the presence of 12 pairs of ribs in all three Stim1$^{R304W/R304W}$ mice (Fig. 1C), which is in contrast to the 13 pairs of ribs in wild type mice. No other abnormal features were observed on X-ray. Thoracic kyphosis was not detected by macroscopic examination of 91 heterozygous Stim1$^{R304W/+}$ mice. Further micro-computed tomography (μCT) scans and data analysis did not detect differences in the femur to tibia length ratios in the homozygous mice compared to wild type (data not shown). Therefore, the X-ray and μCT results indicated that the skeleton of the Stim1$^{R304W/R304W}$ mice were smaller, but proportionate in comparison to the wild type mice.

3.2. Patients with the STIM1 R304W mutation did not present with clear skeletal anomalies

Motivated by the skeletal anomalies in the Stim1^{R304W} mouse line, we did a retrospective analysis on chest X-ray and CT scans in six patients with Stormorken syndrome [13,14,33]. We did not detect skeletal abnormalities in ribs and spine in patient F1 III-1 and F3 II-1 reported by Misceo et al., [13], in patient F1 III-2 described by Nesin et al., [14], and in the patient described by Borsani et al., [33]. Patient F2 II-3 in Misceo et al. [13], also had a normal spine and normal number of pairs of ribs, but rib number 5 on the right side was bifid anteriorly, and presented with periarticular soft tissue calcifications. Patient F4 III-1 in Misceo et al., [13] had normal vertebrae and number of ribs, but showed a slight thoracic scoliosis of about 25°. Bone density was considered normal in all patients evaluated by CT and or X-ray radiographs, including normal thickness of the cortical bone. However, it should be noted that these patients maintain a wild type *STIM1* allele, in contrast to the mice that are homozygous for the Stormorken mutation, which thus are expected to have a more severe phenotype. The subtle skeletal features in these patients call for examination of more patients with Stormorken syndrome or other GoF STIM1 mutations to assess for the presence of skeletal anomalies.

3.3. Abnormal bone architecture in the Stim1^{R304W} mouse line

Macroscopic examinations of cross sections of the femurs revealed normal bone marrow cavity in the wild type mice, but narrow, almost absent bone marrow cavity in the three Stim1$^{R304W/R304W}$ mice.

In the Stim1$^{R304W/R304W}$ mice μCT analyses of the tibiae documented pathogenic changes in trabecular and cortical bone architecture compared to age and sex matched wild type mice (Fig. 2A–I). The homozygous mice showed significantly decreased trabecular separation ($p < 0.05$), increased trabecular bone volume fraction ($p < 0.05$) and trabecular number ($p < 0.05$) (Fig. 2D–F) compared to wild type mice. They also showed a decrease in mean total cross-sectional cortical bone area ($p < 0.05$), cortical bone volume ($p < 0.05$) and cortical bone surface area ($p < 0.05$) (Fig. 2G–I). The heterozygous mice showed an intermediate phenotype between the wild type and the homozygous mice (Fig. 2D–F). Thus, the Stim1^{R304W} mouse line presented with pathological features in the skeletal system, which includes decreased cortical bone volume and an increased trabecular bone volume fraction, with thinner and more compact trabeculae (Fig. 2A–I).

Histological examination of HE stained sections of the proximal segment of the tibial diaphysis of wild type mice showed normal ossification with slender bone trabeculae and an abundant bone marrow. In contrast, the Stim1$^{R304W/R304W}$ mice presented with reduced bone marrow cavity, resulting in a more compact morphology (Fig. 3A–D).

3.4. STIM1 R304W was expressed in megakaryocytes, osteoblasts and osteocytes

The expression of the STIM1 protein in bone was assessed by IHC on bone sections from tibiae of homozygous and wild type mice. The data showed that the osteoblasts lining the bone trabeculae and the osteocytes embedded in the bone matrix were strongly positive for STIM1 in both wild type and Stim1$^{R304W/R304W}$ mice (Fig. 3E and F).

We previously documented lack of STIM1 protein in platelets from the Stim1$^{R304W/R304W}$→WT chimeras and in embryonic liver megakaryocytes from the Stim1$^{R304W/R304W}$ mice [29]. In the only three Stim1$^{R304W/R304W}$ mice surviving to adulthood, however, bone marrow megakaryocytes stained positive for STIM1 by IHC (Fig. 4). Thus, the mutant protein was detected in the hematopoietic lineage in all the three Stim1$^{R304W/R304W}$ mice surviving to adulthood.

3.5. Stim1$^{R304W/R304W}$ mice presented with splenomegaly

Stim1$^{R304W/R304W}$ mice presented splenomegaly and showed a mean spleen to body mass ratio of 0.0125 ($n = 3$) while WT was 0.00275 ($n = 18$) ($p < 0.005$) (Fig. 5). Splenomegaly is observed in mice with impaired bone marrow activity [34], and was also detected in the *Stim1*^{R304W} mice described by Silva-Rojas et al. [31].

3.6. The Stim1^{R304W} mouse line presented with bilateral subgingival hair growth on the lower incisors

All three homozygous Stim1$^{R304W/R304W}$ mice presented with hair originating from the labial side of the lower incisors, which became evident within the first two months of life (Fig. 6A). Similar ectopic subgingival hair growth on the lower incisors was also detected in 18/70 (26 %) of the heterozygous Stim1$^{R304W/+}$ mice examined.

The color and structure of the incisors of the Stim1$^{R304W/R304W}$ mice was comparable to the wild type littermates. The incisors did not have a 'chalky' appearance, which could have indicated abnormal mineralization. Cross sections of incisor enamel from one wild type and one Stim1$^{R304W/R304W}$ mouse were imaged in BSE-SEM to assess broad differences in mineralization of the enamel. Wild type and Stim1$^{R304W/R304W}$ mice did not show significant mineralization differences (Fig. 6B–C). Together, these data point to a defect in epithelial cell fate in Stim1^{R304W} mouse line, not previously described in mice with *Stim1* or *Orai1* mutations.

4. Discussion

Store-operated calcium channels (SOCE) serve as a main Ca^{2+} regulating mechanism in both bone and dental tissue growth and development in man and mouse. This is evident in patients with Ca^{2+} release-activated Ca^{2+} (CRAC) channelopathies, who present with defects in dental enamel mineralization [8]. A dental phenotype with chalky enamel is also observed in *Stim1*-deficient mice [35,36]. In the bone, ORAI1 regulates osteoblast and osteoclast formation and differentiation [37]. The role of STIM1 in these processes is less understood [38]. However, based on the importance of SOCE, it can be hypothesized that STIM1 also plays a critical role in these processes and any disruption in STIM1 function may result in imbalances of bone homeostasis and in dental enamel formation. The Stim1^{R304W} mouse model demonstrates that constitutive SOCE due to the GoF *Stim1* mutation results in skeletal defects and abnormal epithelial cell fate, thereby making Stim1^{R304W} mice a tool for exploring the effects of constitutive SOCE induced Ca^{2+} dysregulation in these tissues.

STIM1 GoF mutations are pathogenic in mice, but the cellular and phenotypic effects seem to be different for each mutation [29–31]. Embryonic lethality at < 14.5 dpc caused by severe bleeding is described in mice expressing the EF-hand GoF mutation STIM1 D84G [30], while homozygous Stim1 R304W mice died perinatally with no signs of bleeding [29]. STIM1 is important in muscle at early developmental stages [39,40], and both the heterozygous Stim1 $^{R304W/+}$ mice and the surviving homozygotes showed severe skeletal muscle degeneration [29], indicating that the cause of lethality may be understood by further studies of the muscle pathology in our Stim1^{R304W} mice.

Our Stim1^{R304W} mice showed macroscopic skeletal anomalies: proportionally small skeleton, reduced number of ribs and kyphosis in Stim1$^{R304W/R304W}$ mice. We further documented severe microscopic anomalies in the bone architecture of these mice, with increased trabecular to cortical bone fraction, and almost absent bone marrow cavity. This is in line with the observations in the mouse model described by Silva-Rojas et al. [31], expressing the same mutation, which presented with decreased cellular density, reduced bone marrow cavity and abnormal mechanical bone properties. In contrast, re-analysis of X-ray and CT scans of six patients with Stormorken syndrome expressing

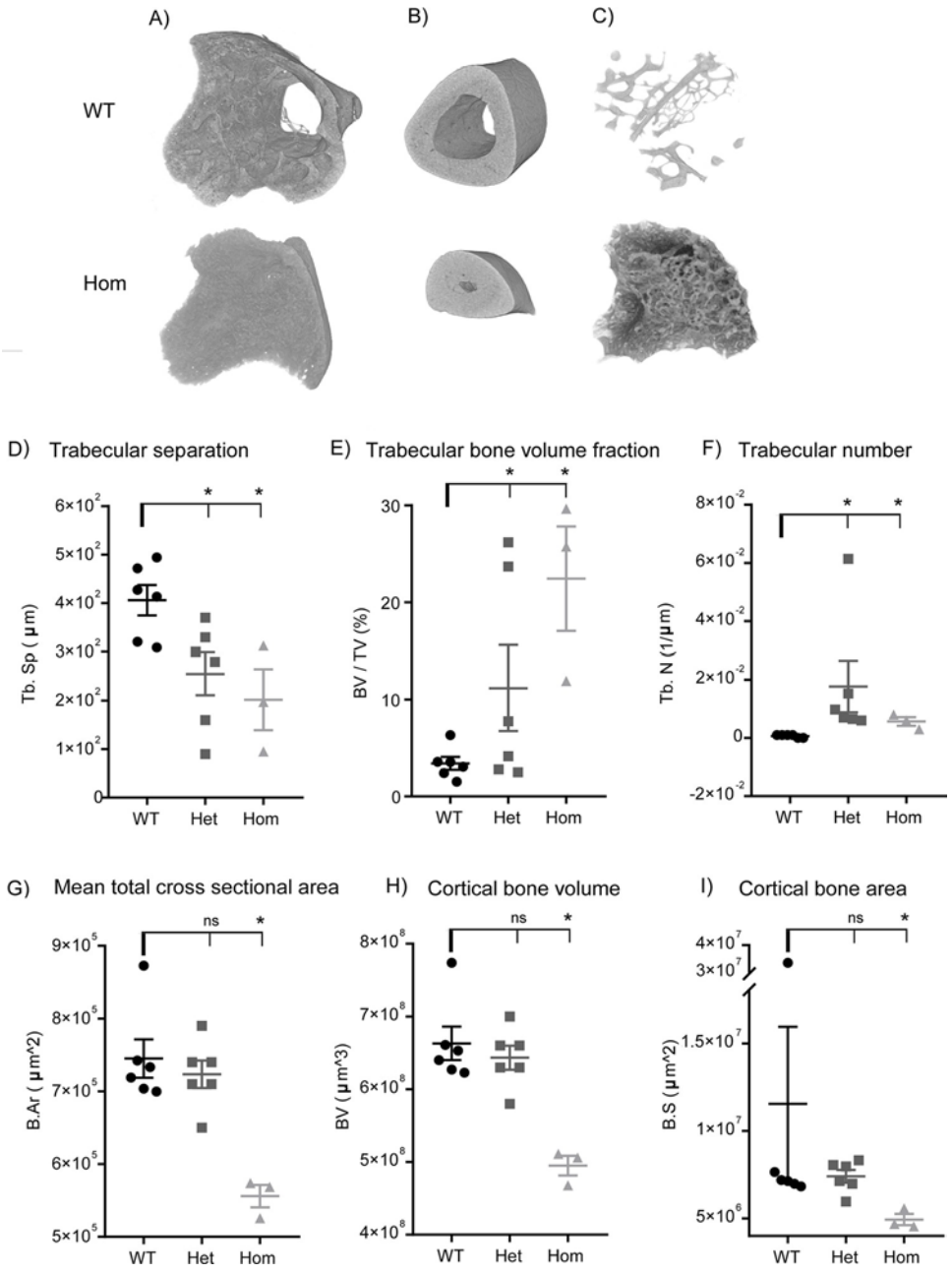

Fig. 2. µCT analyses of the tibia showed increased trabecular to cortical bone fraction in Stim1^{R304W} mice.

(A–C) 3D projections of µCT scanning of tibia from Stim1$^{R304W/R304W}$ and wild type mice as indicated. Homozygous mice presented decreased cortical bone volume (B) and increased trabecular bone volume fraction with thinner and more compact trabeculae (C) compared to the wild types.

(D–I) Homozygous mice (n = 3) presented with significantly decreased trabecular separation (D), increased trabecular bone volume fraction (E) and trabecular number (F) compared to wild type mice (n = 6). Significantly decreased mean total cross sectional area (G), cortical bone volume (H) and cortical bone area (I) were also seen in Stim1$^{R304W/R304W}$ mice (n = 3) in comparison to age matched wild type mice (n = 6). Heterozygous Stim1^{R304W} mice (n = 6) showed an intermediate phenotype between wild type and homozygous littermates in all aspects above (D–F).

In all panels, p-values for significance are indicated as *=p < 0.05.

B.Ar: bone area; B.S: bone volume fraction; BV: bone volume; BV/TV: bone volume/trabecular volume; Het: heterozygous; Hom: homozygous; Tb. N: trabecular number; Tb. Sp: trabecular separation; WT: wild type.

the STIM1 R304W mutation detected only minor and varied anomalies, which may also be observed in otherwise healthy individuals. Skeletal examination of additional patients with Stormorken syndrome is needed to assess if *STIM1* GoF mutations cause skeletal anomalies in humans.

We previously showed that STIM1 expression was reduced or undetectable in megakaryocytes and platelets of our heterozygous and homozygous Stim1^{R304W} mice at embryonic stages and in fetal liver chimeras [29]. However, the three homozygous Stim1^{R304W} mice surviving to adulthood showed STIM1 expression in bone marrow megakaryocytes (Fig. 4), documenting expression of the mutant protein in the hematopoietic lineage. Osteoclasts also originate from hematopoietic stem cells, which differentiate to form monocyte precursors that subsequently fuse into mature multinucleated osteoclasts, which mediate bone resorption by decalcifying and degrading the bone matrix [41]. ORAI1 and STIM1 are required for the mononuclear osteoclast fusion, a vital step of the late osteoclast differentiation [42], and *Orai1* KO mice show reduced trabecular thickness and reduced cortical ossification [26]. The Stim1^{R304W} mice, however, showed increased trabecular bone volume and number. Because the hematopoietic cells of adult homozygous Stim1^{R304W} mice showed STIM1 expression and because the bone phenotype of homozygous and heterozygous Stim1^{R304W} mice differed from the phenotype of mice lacking ORAI1, it is reasonable to postulate that the mutant STIM1 is also expressed in the osteoclasts in the adult homozygous Stim1^{R304W} mice.

Osteoblasts, which secrete matrix proteins necessary for bone mineralization, originate from mesenchymal stem cells in the bone marrow [43,44]. STIM1 is highly expressed in pre-osteoblasts [44], where Ca^{2+} signaling is essential for their differentiation into mature osteoblasts [45]. We documented expression of the mutant STIM1 R304W protein in the osteoblasts in the homozygous Stim1^{R304W} mice. However, more studies are required into the development and function of both osteoblasts and osteoclasts associated with CRAC channel function to understand the exact mechanism and cell type affected in our Stim1^{R304W} mice leading to the pathogenic phenotype.

Mice naturally have an insufficient total bone marrow volume, and

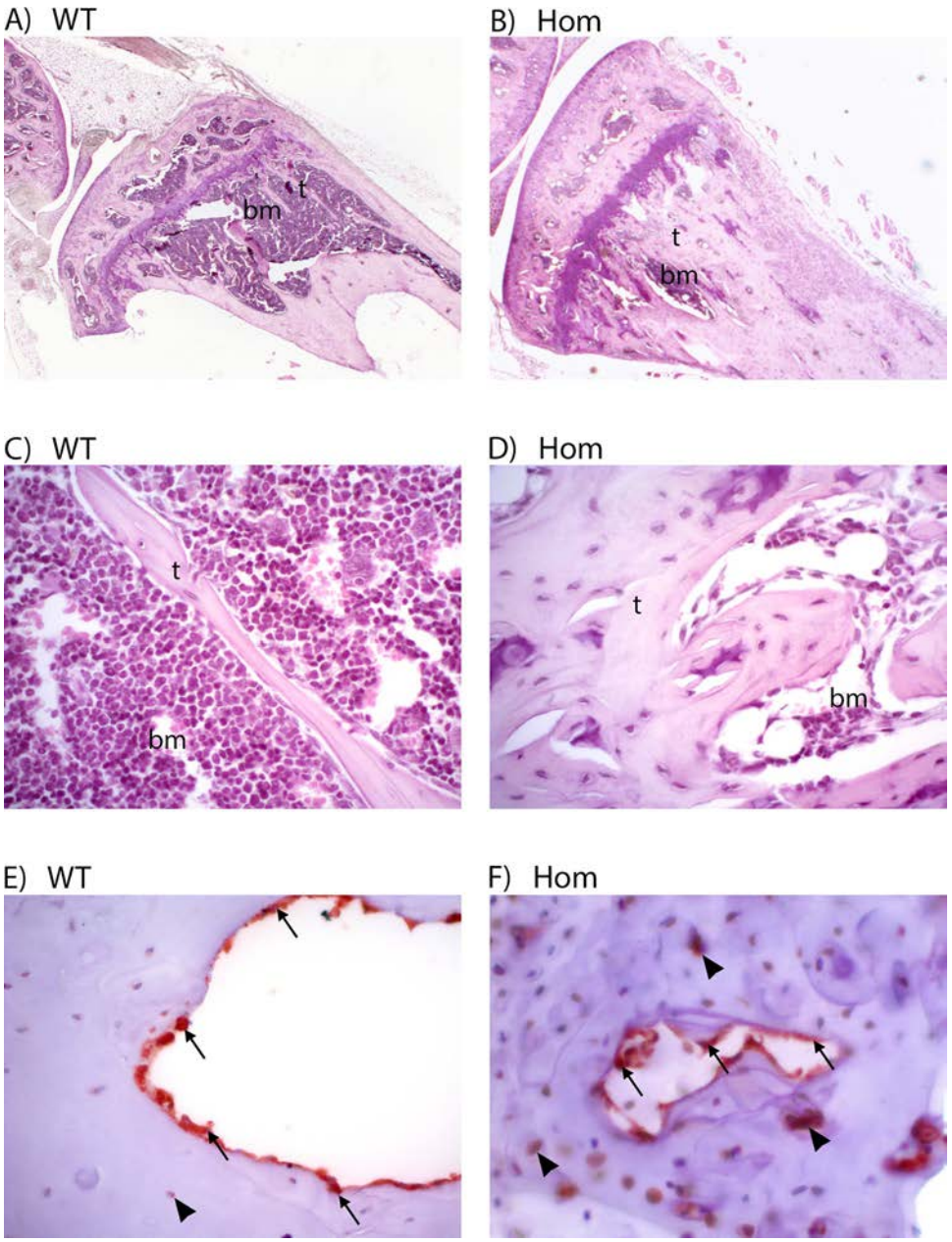

Fig. 3. HE and IHC staining of sections of proximal tibia from Stim1$^{R304W/R304W}$ and wild type mice.
(A–B) Ossification of the proximal tibia of age matched wild type (WT) and Stim1$^{R304W/R304W}$ (Hom) mice.
Wild type mice showed normal ossification with slender bone trabeculae and abundant bone marrow (A), while Stim1$^{R304W/R304W}$ consistently show increased bone mass with broad bone trabeculae and relatively sparse bone marrow by HE staining (B) (magnification 25×).
(C–D) HE stained sections of the proximal tibia from a wild type and Stim1$^{R304W/R304W}$, respectively (magnification 400×).
(E–F) IHC of sections (STIM1) from wild type (E) and *Stim1*$^{R304W/R304W}$ mice (F) showed strongly STIM1 positive osteoblasts (arrows) and embedded osteocytes (arrowheads) (magnification 400×).
bm: bone marrow; t: trabeculae.

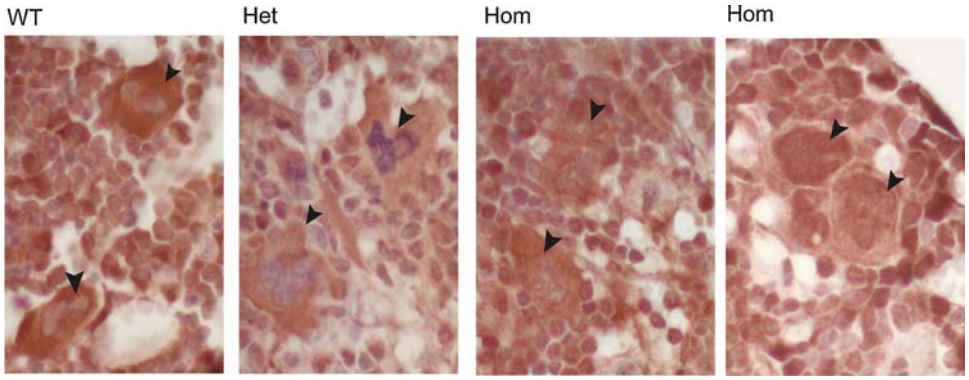

Fig. 4. STIM1 staining in megakaryocytes from bone marrow of Stim1$^{R304W/R304W}$ mice.
IHC of bone marrow showed STIM1 expression in megakaryocytes in adult wild type, Stim1$^{R304W/+}$ and Stim1$^{R304W/R304W}$ mice (n = 2) (arrowheads) (Magnification: 400x).
Het: heterozygous; Hom: homozygous; WT: wild type.

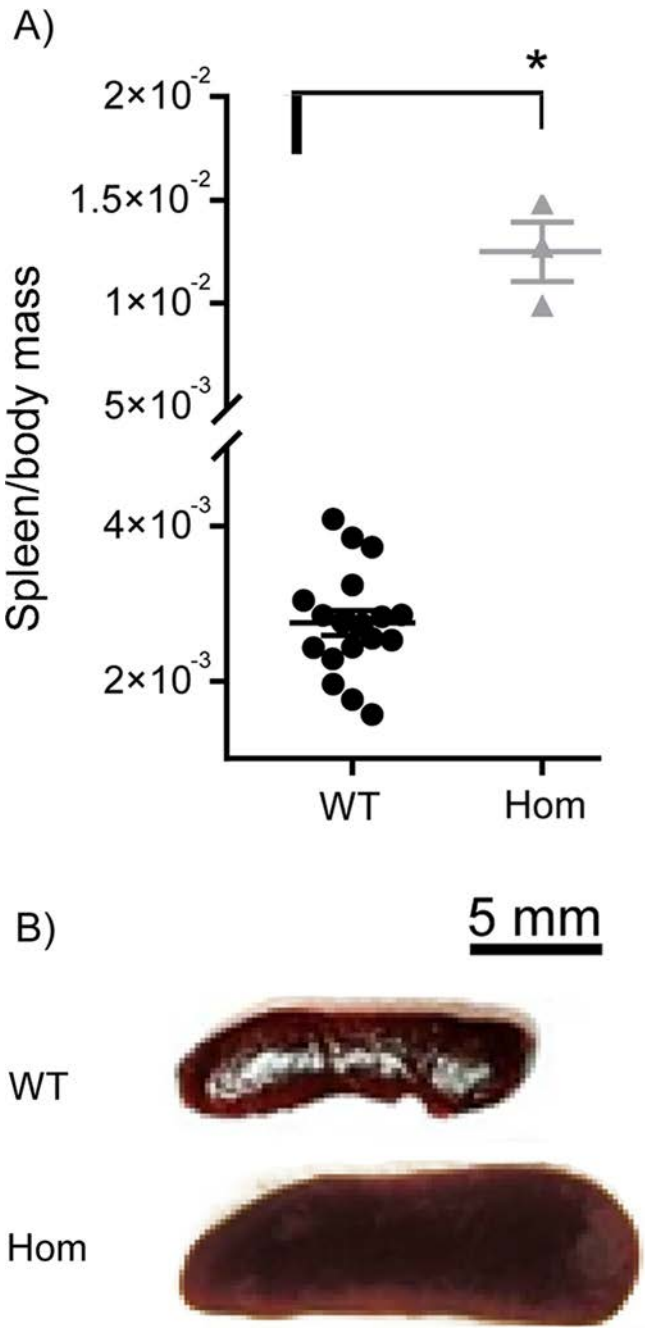

Fig. 5. Stim1^{R304W} homozygous mice presented with splenomegaly.
(A) A significantly increased spleen to body mass ratio was observed in homozygous Stim1^{R304W} mice (n = 3) compared to wild type littermates (n = 18) (*=p < 0.005).
(B) Representative images of dissected spleen from age matched wild type and *Stim1*$^{R304W/R304W}$ mouse as indicated. Hom: homozygous; WT: wild type.

the murine spleen is an essential extension of the hematopoietic organ [34]. Furthermore, impaired bone marrow activity causes enlargement of the spleen in mice due to a higher demand of spleen functionality [34]. In line with this, the homozygous Stim1^{R304W} mice showed splenomegaly and a reduced bone marrow cavity with less abundant bone marrow. Similar observations of splenomegaly in parallel with bone marrow reduction were reported in the *Stim1*^{Sax} mouse model [30] and in the *Stim1*^{R304W} mouse model reported by Silva-Rojas et al. [31].

Impaired SOCE in enamel cells in mice, due to lack of *Stim1* caused hypo-mineralized, thin and mechanically weak enamel, with reduced Ca^{2+} content [35,36]. However the effect of increased SOCE activity due to overactive STIM1 in dental enamel in mice is not described. Expression of the GoF STIM1 R304W mutation in our Stim^{R304W} mice did not seem to cause obvious mineralization differences when comparing to wild type animals by BSE-SEM of incisor enamel. This is in line with the previously reported observation of normal enamel mineralization in mice with increased SOCE due to knock-down of *Orai2* [25]. Together these observations indicate that lack of SOCE has more substantial pathogenic impact on the enamel mineralization than constitutive SOCE in mice.

The ectopic subgingival hair structures in the Stim1^{R304W} mice do not seem to replace enamel growth, but are rather generated in addition to the normal enamel. Rodent incisors have a stem cell compartment at the base (the cervical loop) enabling continuous growth of the tooth, as cells differentiate into different cell types including ameloblasts [46]. Tooth morphogenesis is similar to that of hair and other ectodermal tissues [46], but hair growth in gingiva is uncommon. However, a similar ectopic hair growth as described in our Stim1^{R304W} mice was reported in the epithelium specific mediator complex subunit 1 (*Med1*) knock-out mouse model [47]. Yoshizaki et al. [47] suggested that in these mice the lack of *Med1* caused reduced Notch signaling; a pathway which regulates cell fate in different tissues including the dental epithelial cells [48]. With reduced Notch signaling, the dental epithelia converted into epidermal epithelia due to failure in committing to a dental lineage. This in turn caused defects in the development of enamel, while promoting hair growth in *Med1* KO mice [47,48]. Furthermore, epidermal fate is induced by Ca^{2+} [47]. However, elevated Ca^{2+} is also known to downregulate Notch signaling causing defects in cell lineage commitment [49]. Thus, dysregulation of the Ca^{2+} driven epithelial cell fate may be the cause of the ectopic hair growth in the Stim1^{R304W} mice. The ectopic subgingival hair development suggest a potential suppression of the Notch pathway in *Stim1*$^{R304W/R304W}$ mice. It is tempting to hypothesize that a similar suppression of the Notch pathway in mesenchymal progenitor cells, osteoblasts, osteocytes and/or osteoclasts, which express STIM1 and are all known to be affected by the Notch signaling [50], could explain part of the skeletal phenotype of these mice.

5. Conclusion

The Stim1^{R304W} mouse line presented a skeletal phenotype characterized by significant pathogenicity in trabecular and cortical bone, kyphosis, reduced number of ribs, and reduced bone marrow cavity. In addition, the mice showed splenomegaly and ectopic growth of subgingival hair possibly caused by a defect in epithelial cell fate. Our data further confirm the previous reports that elevated SOCE does not seem to affect enamel mineralization [25], but cause severe defects in bone architecture in mice [30,31]. This further highlights the importance of the ER-protein STIM1 in skeletal system development and homeostasis. Further studies of the osteoclasts, osteoblasts, ameloblasts and epithelial stem cells expressing the mutant STIM1 R304W protein may reveal the dysregulated molecular pathways that cause the observed abnormalities in the Stim1^{R304W} mouse line.

Declaration of Competing Interest

There are no conflicts of interests to declare.

Acknowledgements

We are grateful to the patients who participated in this study. E.L. received a stipend from the Research Council of Norway, project number 271555/F20, through the Medical Student Research Program. T.G. was supported financially by the Quota scheme of Norwegian State Educational Loan Fund, “Mobility grant for PhD students by the Institute for Clinical medicine”, University of Oslo and by UNIFOR.

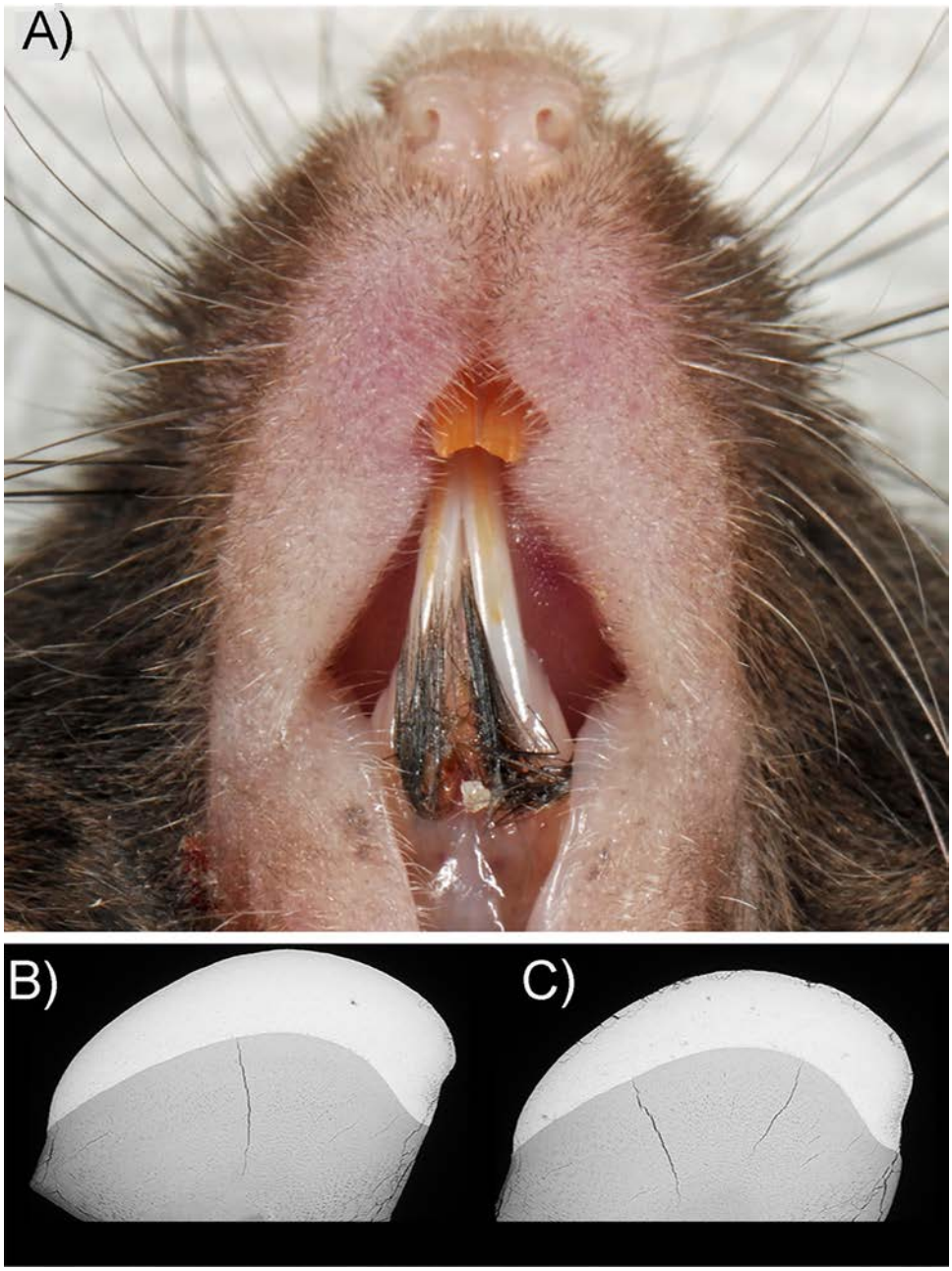

Fig. 6. Ectopic subgingival hair growth in the Stim1^{R304W} mouse line.
(A) Representative image from a $Stim1^{R304W/R304W}$ mouse shows bilateral ectopic hair growth from the labial side of the lower incisors appearing to originate from the gingiva. Macroscopic enamel morphology appeared normal, without chalky appearance.
(B–C) BSE-SEM of cross section of incisors did not reveal differences in signals (brightness) between the wild type (B) and the $Stim1^{R304W/R304W}$ mouse (C).

References

[1] H.C. Blair, L.J. Robinson, C.L. Huang, et al., Calcium and bone disease, Biofactors 37 (2011) 159–167.
[2] J.W. Putney Jr., A model for receptor-regulated calcium entry, Cell Calcium 7 (1986) 1–12.
[3] J.W. Putney Jr., New molecular players in capacitative Ca2+ entry, J. Cell. Sci. 120 (2007) 1959–1965.
[4] J. Liou, M.L. Kim, W.D. Heo, et al., STIM is a Ca2+ sensor essential for Ca2+-store-depletion-triggered Ca2+ influx, Curr. Biol. 15 (2005) 1235–1241.
[5] R.M. Luik, B. Wang, M. Prakriya, M.M. Wu, R.S. Lewis, Oligomerization of STIM1 couples ER calcium depletion to CRAC channel activation, Nature 454 (2008) 538–542.
[6] S.L. Zhang, Y. Yu, J. Roos, et al., STIM1 is a Ca2+ sensor that activates CRAC channels and migrates from the Ca2+ store to the plasma membrane, Nature 437 (2005) 902–905.
[7] R.M. Luik, M.M. Wu, J. Buchanan, R.S. Lewis, The elementary unit of store-operated Ca2+ entry: local activation of CRAC channels by STIM1 at ER-plasma membrane junctions, J. Cell Biol. 174 (2006) 815–825.
[8] R.S. Lacruz, S. Feske, Diseases caused by mutations in ORAI1 and STIM1, Ann. N. Y. Acad. Sci. 1356 (2015) 45–79.
[9] S. Feske, Y. Gwack, M. Prakriya, et al., A mutation in Orai1 causes immune deficiency by abrogating CRAC channel function, Nature 441 (2006) 179–185.
[10] J. Bohm, F. Chevessier, A. Maues De Paula, et al., Constitutive activation of the calcium sensor STIM1 causes tubular-aggregate myopathy, Am. J. Hum. Genet. 92 (2013) 271–278.
[11] Y. Endo, S. Noguchi, Y. Hara, et al., Dominant mutations in ORAI1 cause tubular aggregate myopathy with hypocalcemia via constitutive activation of store-operated Ca(2)(+) channels, Hum. Mol. Genet. 24 (2015) 637–648.
[12] S. Feske, CRAC channelopathies, Pflugers Arch. 460 (2010) 417–435.
[13] D. Misceo, A. Holmgren, W.E. Louch, et al., A dominant STIM1 mutation causes Stormorken syndrome, Hum. Mutat. 35 (2014) 556–564.
[14] V. Nesin, G. Wiley, M. Kousi, et al., Activating mutations in STIM1 and ORAI1 cause overlapping syndromes of tubular myopathy and congenital miosis, Proc. Natl. Acad. Sci. U. S. A. 111 (2014) 4197–4202.
[15] C. Picard, C.A. McCarl, A. Papolos, et al., STIM1 mutation associated with a

syndrome of immunodeficiency and autoimmunity, N. Engl. J. Med. 360 (2009) 1971–1980.
[16] C.A. McCarl, C. Picard, S. Khalil, et al., ORAI1 deficiency and lack of store-operated Ca2+ entry cause immunodeficiency, myopathy, and ectodermal dysplasia, J. Allergy Clin. Immunol. 124 (2009) 1311–1318 e1317.
[17] S. Fuchs, A. Rensing-Ehl, C. Speckmann, et al., Antiviral and regulatory T cell immunity in a patient with stromal interaction molecule 1 deficiency, J. Immunol. 188 (2012) 1523–1533.
[18] G. Morin, N.O. Bruechle, A.R. Singh, et al., Gain-of-Function mutation in STIM1 (P.R304W) is associated with stormorken syndrome, Hum. Mutat. 35 (2014) 1221–1232.
[19] J. Bohm, F. Chevessier, C. Koch, et al., Clinical, histological and genetic characterisation of patients with tubular aggregate myopathy caused by mutations in STIM1, J. Med. Genet. 51 (2014) 824–833.
[20] H. Stormorken, H. Holmsen, R. Sund, et al., Studies on the haemostatic defect in a complicated syndrome. An inverse Scott syndrome platelet membrane abnormality? Thromb. Haemost. 74 (1995) 1244–1251.
[21] O. Sjaastad, J. Aasly, H. Stormorken, M.M. Wysocka-Bakowska, I. Horven, T.A. Fredriksen, A new hereditary syndrome with a bleeding tendency, extreme miosis, spasms, dyslexia, thrombocytopathia etc. Pupillometric, evaporimetric, and ophthalmological observations, Acta Ophthalmol. (Copenh.) 70 (1992) 713–720.
[22] M. Mizobuchi, C. Tanaka, K. Sako, et al., Muscle involvement of Stormorken's syndrome, Rinsho Shinkeigaku 40 (2000) 915–920.
[23] T. Markello, D. Chen, J.Y. Kwan, et al., York platelet syndrome is a CRAC channelopathy due to gain-of-function mutations in STIM1, Mol. Genet. Metab. 114 (2015) 474–482.
[24] A. Braun, D. Varga-Szabo, C. Kleinschnitz, et al., Orai1 (CRACM1) is the platelet SOC channel and essential for pathological thrombus formation, Blood 113 (2009) 2056–2063.
[25] M. Eckstein, M. Vaeth, F.J. Aulestia, et al., Differential regulation of Ca(2+) influx by ORAI channels mediates enamel mineralization, Sci. Signal. 12 (2019).
[26] L.J. Robinson, S. Mancarella, D. Songsawad, et al., Gene disruption of the calcium channel Orai1 results in inhibition of osteoclast and osteoblast differentiation and impairs skeletal development, Lab. Invest. 92 (2012) 1071–1083.
[27] J. Stiber, A. Hawkins, Z.S. Zhang, et al., STIM1 signalling controls store-operated calcium entry required for development and contractile function in skeletal muscle, Nat. Cell Biol. 10 (2008) 688–697.
[28] D. Varga-Szabo, A. Braun, C. Kleinschnitz, et al., The calcium sensor STIM1 is an essential mediator of arterial thrombosis and ischemic brain infarction, J. Exp. Med. 205 (2008) 1583–1591.
[29] T.H. Gamage, G. Gunnes, R.H. Lee, et al., STIM1 R304W causes muscle degeneration and impaired platelet activation in mice, Cell Calcium 76 (2018) 87–100.
[30] J. Grosse, A. Braun, D. Varga-Szabo, et al., An EF hand mutation in Stim1 causes premature platelet activation and bleeding in mice, J. Clin. Invest. 117 (2007) 3540–3550.
[31] R. Silva-Rojas, S. Treves, H. Jacobs, et al., STIM1 over-activation generates a multisystemic phenotype affecting the skeletal muscle, spleen, eye, skin, bones and immune system in mice, Hum. Mol. Genet. 28 (2019) 1579–1593.
[32] M. Eckstein, M. Vaeth, C. Fornai, et al., Store-operated Ca(2+) entry controls ameloblast cell function and enamel development, JCI Insight 2 (2017) e91166.
[33] O. Borsani, D. Piga, S. Costa, et al., Stormorken syndrome caused by a p.R304W STIM1 mutation: the first italian patient and a review of the literature, Front. Neurol. 9 (2018) 859.
[34] W.H. Crosby, Hematopoiesis in the human spleen, Arch. Intern. Med. 143 (1983) 1321–1322.
[35] M. Eckstein, F.J. Aulestia, M.K. Nurbaeva, R.S. Lacruz, Altered Ca(2+) signaling in enamelopathies, Biochim. Biophys. Acta Mol. Cell Res. 1865 (2018) 1778–1785.
[36] Y. Furukawa, N. Haruyama, M. Nikaido, et al., Stim1 regulates enamel mineralization and ameloblast modulation, J. Dent. Res. 96 (2017) 1422–1429.
[37] L.J. Robinson, S. Mancarella, I.L. Tourkova, J.B. Barnett, H.C. Blair, J. Soboloff, Critical role for the calcium-release activated calcium channel Orai1 in RANKL-Stimulated osteoclast formation from, Monocytic Cells 116 (2010) 928-928.
[38] S.Y. Hwang, J. Foley, T. Numaga-Tomita, J.G. Petranka, G.S. Bird, J.W. Putney Jr., Deletion of Orai1 alters expression of multiple genes during osteoclast and osteoblast maturation, Cell Calcium 52 (2012) 488–500.
[39] S. Mancarella, S. Potireddy, Y. Wang, et al., Targeted STIM deletion impairs calcium homeostasis, NFAT activation, and growth of smooth muscle, FASEB J. 27 (2013) 893–906.
[40] T. Li, E.A. Finch, V. Graham, et al., STIM1-Ca(2+) signaling is required for the hypertrophic growth of skeletal muscle in mice, Mol. Cell. Biol. 32 (2012) 3009–3017.
[41] T. Negishi-Koga, H. Takayanagi, Ca2+-NFATc1 signaling is an essential axis of osteoclast differentiation, Immunol. Rev. 231 (2009) 241–256.
[42] Y. Zhou, T.L. Lewis, L.J. Robinson, et al., The role of calcium release activated calcium channels in osteoclast differentiation, J. Cell. Physiol. 226 (2011) 1082–1089.
[43] M.F. Pittenger, A.M. Mackay, S.C. Beck, et al., Multilineage potential of adult human mesenchymal stem cells, Science 284 (1999) 143–147.
[44] Y. Chen, A. Ramachandran, Y. Zhang, R. Koshy, A. George, The ER Ca(2+) sensor STIM1 can activate osteoblast and odontoblast differentiation in mineralized tissues, Connect. Tissue Res. 59 (2018) 6–12.
[45] A. Eapen, P. Sundivakkam, Y. Song, et al., Calcium-mediated stress kinase activation by DMP1 promotes osteoblast differentiation, J. Biol. Chem. 285 (2010) 36339–36351.
[46] M. Jussila, I. Thesleff, Signaling networks regulating tooth organogenesis and regeneration, and the specification of dental mesenchymal and epithelial cell lineages, Cold Spring Harb. Perspect. Biol. 4 (2012) a008425.
[47] K. Yoshizaki, L. Hu, T. Nguyen, et al., Ablation of coactivator Med1 switches the cell fate of dental epithelia to that generating hair, PLoS One 9 (2014) e99991.
[48] T.A. Mitsiadis, D. Graf, H. Luder, T. Gridley, G. Bluteau, BMPs and FGFs target Notch signalling via jagged 2 to regulate tooth morphogenesis and cyto differentiation, Development 137 (2010) 3025–3035.
[49] J.P. Eid, A.M. Arias, H. Robertson, G.R. Hime, M. Dziadek, The Drosophila STIM1 orthologue, dSTIM, has roles in cell fate specification and tissue patterning, BMC Dev. Biol. 8 (2008) 104.
[50] D.W. Youngstrom, K.D. Hankenson, Contextual regulation of skeletal physiology by notch signaling, Curr. Osteoporos. Rep. 17 (2019) 217–225.